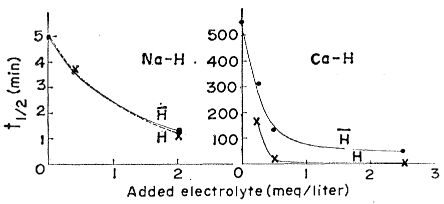

Fig. 2. Half time of exchange between Na or Ca from montmorillonite suspension and H from Amberlite IR-120 at different electrolyte concentrations. $\bar{H}$, in clay; H, in supernatant solution.

exchange between Na or Ca on the montmorillonite and H in the supernatant, $t_{1/2}$ may be given (*4*) by

$$t_{1/2} = (0.167 + 0.064\, \alpha_{\mathrm{H}}{}^{\mathrm{M}}) \frac{r\delta\bar{c}}{Dc} \qquad (2)$$

where $\alpha_{\mathrm{H}}{}^{\mathrm{M}}$ is the separation factor for exchange of the metallic ion for hydrogen, r is the particle radius, δ is the thickness of the Nernst layer, $\bar{c}$ the exchange capacity of the exchanger, D the interdiffusion coefficient in the film, and c the electrolyte concentration in solution. As r and δ for montmorillonite are not known and are difficult to evaluate, no absolute value for $t_{1/2}$ can be calculated. However, it is possible to calculate the ratio $t_{1/2}$(Ca-H)/$t_{1/2}$(Na-H) with δ (which mainly depends on the stirring conditions), $\bar{c}$, and c equal for the two ionic states, with known values for $\alpha_{\mathrm{H}}{}^{\mathrm{M}}$ and D ratios (*5*) and estimated ratios of $r_{\mathrm{Ca}}/r_{\mathrm{Na}}$. The calculated and observed ratios are given in Table 1. A slight slowing is predicted in the Ca-H exchange relative to the Na-H exchange even if the montmorillonite particle size is the same in the two ionic states. This is due to the smaller diffusion coefficient of the Ca ion and the higher preference of the clay for it. However, most of the observed reduction in rate may be explained if the Ca-montmorillonite particle is about ten times larger than the Na-montmorillonite particle. This can be brought by the adhering of the clay plates, totally separated when in the Na state, to form tactoids, containing about ten plates each, when in the Ca state (*6*).

Table 1. Observed and calculated ratios of half time of exchange between Na or Ca on montmorillonite and H on Amberlite IR-120.

Electrolyte conc. (meq/liter)	Observed $t_{1/2}$(min) (Ca-H)	Observed $t_{1/2}$(min) (Na-H)	$t_{1/2}$(Ca-H) / $t_{1/2}$(Na-H)
0.5	135	3.4	40
1.0	85	2.3	37
2.0	50	1.3	38

Calculated

$r_{\mathrm{Ca}}/r_{\mathrm{Na}}$*	$t_{1/2}$(Ca-H)/$t_{1/2}$(Na-H)
1	3.7
5	19
10	37
20	74

* Estimated ratios of particle size of montmorillonite in the Ca and Na states, respectively.

The clay-resin system described above can be used as a model for the soil-plant root system. Ion exchange between H from the root and metallic cations adsorbed on clay particles in the soil is taking place as part of the nutrient uptake process by the plant. Since the soil solution is not stirred, and usually has low electrolyte concentration, film kinetics probably prevails in this exchange reaction. In this case, as the results for the clay-resin systems show, a considerable difference between the rates of the H-divalent and the H-monovalent exchange reactions exists when montmorillonite is present as the main clay mineral. The difference in rate will affect the composition of the ionic flux reaching the root in exchange for its secreted hydrogen and cause what might be called a "kinetic selection," which tends to increase the fraction of monovalent ions adsorbed by the plant (*7*).

AMOS BANIN

Department of Soil Science, Hebrew University, Rehovot, Israel

References and Notes

1. H. Van Olphen, in *Clays and Clay Minerals, 4th Conference* (National Academy of Sciences–National Research Council Publication No. 456, Washington, D.C., 1956), p. 204; in *Clays and Clay Minerals, 6th Conference* (Pergamon, New York, 1959), p. 196; L. A. G. Aylmore and J. P. Quirk, *Nature* **183**, 1752 (1959); *ibid.* **187**, 1046 (1960); in *Clays and Clay Minerals, 9th Conference* (Pergamon, New York, 1962), p. 104; W. W. Emerson, *J. Soil Sci.* **13**, 31, 40 (1962); D. G. Edwards and J. P. Quirk, *J. Colloid Sci.* **17**, 872 (1962).
2. The clay used in this study was the fraction of Wyoming Bentonite (Cenco c-1051) less than 2 μ. The exchange capacity of the clay was 82 meq per 100 g. The resin used was Amberlite IR-120. It had a particle radius range of 0.015 to 0.060 cm and exchange capacity of 4.70 meq per gram.
3. A. Banin and S. Ravikovitch, in *Clays and Clay Minerals, 14th Conference* (Pergamon, New York, 1966), p. 193.
4. F. Helfferich, *Ion Exchange* (McGraw-Hill, New York, 1962), pp. 255, 275.
5. Separation factors were taken at the half-conversion point on the exchange isotherms (A. Banin, in preparation) and were 0.04 and 5.32 for the Na-H and Ca-H exchange reactions, respectively. The ratio of the interdiffusion coefficients in the film was assumed not to differ from the ratio of the diffusion coefficients in solution. Values for the diffusion coefficients of Na and Ca in solution were taken from H. S. Harned and B. B. Owen, *The Physical Chemistry of Electrolytic Solutions* (Reinhold, New York, ed 3, 1958).
6. A. V. Blackmore and R. D. Miller, *Soil Sci. Soc. Am. Proc.* **25**, 169 (1961).
7. Evidence for such a selection can be found in S. Mattson, *Ann. Agr. College Sweden* **12**, 221 (1948); M. M. Elgabaly and L. Wiklander, *Soil Sci.* **67**, 419 (1949); L. Wiklander and M. M. Elgabaly, *ibid.* **80**, 91 (1955).

22 August 1966

Extension of Northeastern-Pacific Fracture Zones

Abstract. *The great fracture zones of the northeastern Pacific extend into the central Pacific. At a relatively constant distance of 4500 to 4900 kilometers west of the crest of the East Pacific Rise and of its projection through North America, the typically straight and simple fracture zones branch and become more complex. However, the Clipperton fracture zone, including one branch, follows a great circle for almost 10,000 kilometers, a quarter of Earth's circumference.*

Recent work has shown that some of the great fracture zones of the northeastern Pacific (*1*) extend beyond the margins of the East Pacific Rise (*2*). The whole pattern of great fractures can be traced far into the central Pacific on recently acquired echograms (*3*) and soundings (*4*).

The Clipperton fracture zone is an outstanding example (Fig. 1), readily traceable as an essentially continuous topographic feature from the crest of the East Pacific Rise to just east of the Line Islands; there it is lost, being apparently buried under the archipelagic apron and volcanoes of the islands as well as the pelagic sediments of the equatorial belt (*5*). It reappears along the same trend south of the equatorial sedimentation belt as a line of troughs, ridges, and changes in regional depth. The relief is generally subdued, but, just east of Enderbury Island in the Phoenix group, an echogram by C.S. *Recorder* shows a trough with a depth of 7300 m, while older spot soundings indicate a maximum depth of 8030 m—by far the greatest known depths in the central Pacific. Bordering the deep trough on the south is a ridge rising to 2330 m and giving a local relief on a steep scarp of 5700 m. The fracture zone continues west along the northern edge of the Phoenix Islands and toward the Gilbert Islands as a band of narrow troughs and ridges with moderate relief. It cannot be found in the vicinity of the Gilberts, although it is quite possibly buried by the archipelagic apron. East of the Line Islands a branch extends westward from the main trend of the fracture zone but cannot be traced beyond the edge of the archipelagic apron; another branch, toward the southwest, exists east of the Phoenix Islands and appears to extend through them. The total known length of the fracture zone

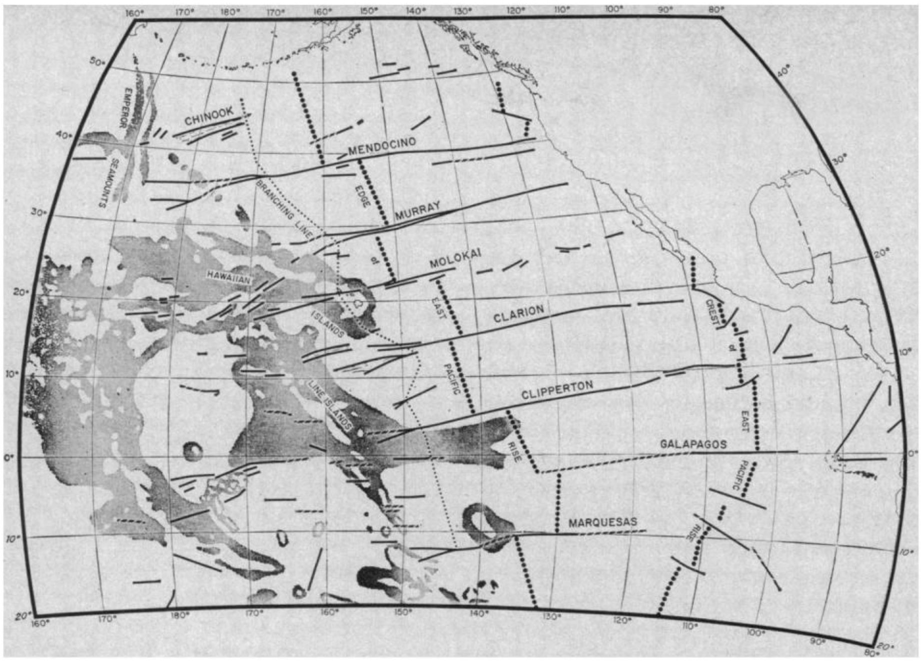

Fig. 1. Principal fracture zones of the northeastern and central Pacific; equal-area projection. Stippling indicates smooth archipelagic aprons and the belt of equatorial pelagic smoothing; white areas within archipelagic aprons are volcanoes and volcanic ridges. Individual lineations are troughs, asymmetric ridges, or regional changes in depth; broken-line bands have fracture-zone topography, but information is not adequate for the tracing of individual lineations.

along a great circle is 9900 km, or about a quarter of the circumference of Earth (Fig. 2).

Many other great fracture zones have been traced for 4000 to 6000 km (Fig. 1) but do not follow great circles over such distances. The most notable exception from a great-circle trend is the Mendocino fracture zone, which changes trend from west to southwest to west and follows the general trend of the other northeastern Pacific zones only in its central portion.

Like the Clipperton zone, the other fracture zones change from predominantly simple lineations in the northeastern Pacific to branching features, with common west and southwest trends, in the central Pacific. The edge of the East Pacific Rise can be defined by the western margin of the sloping flank. Branching occurs west of this margin but at a rather constant distance. On the other hand, if the "ICSU Line," proposed by Wilson (6) on the basis of tectonic arguments to be the edge of the rise, is accepted, the branching occurs on the rise; how-

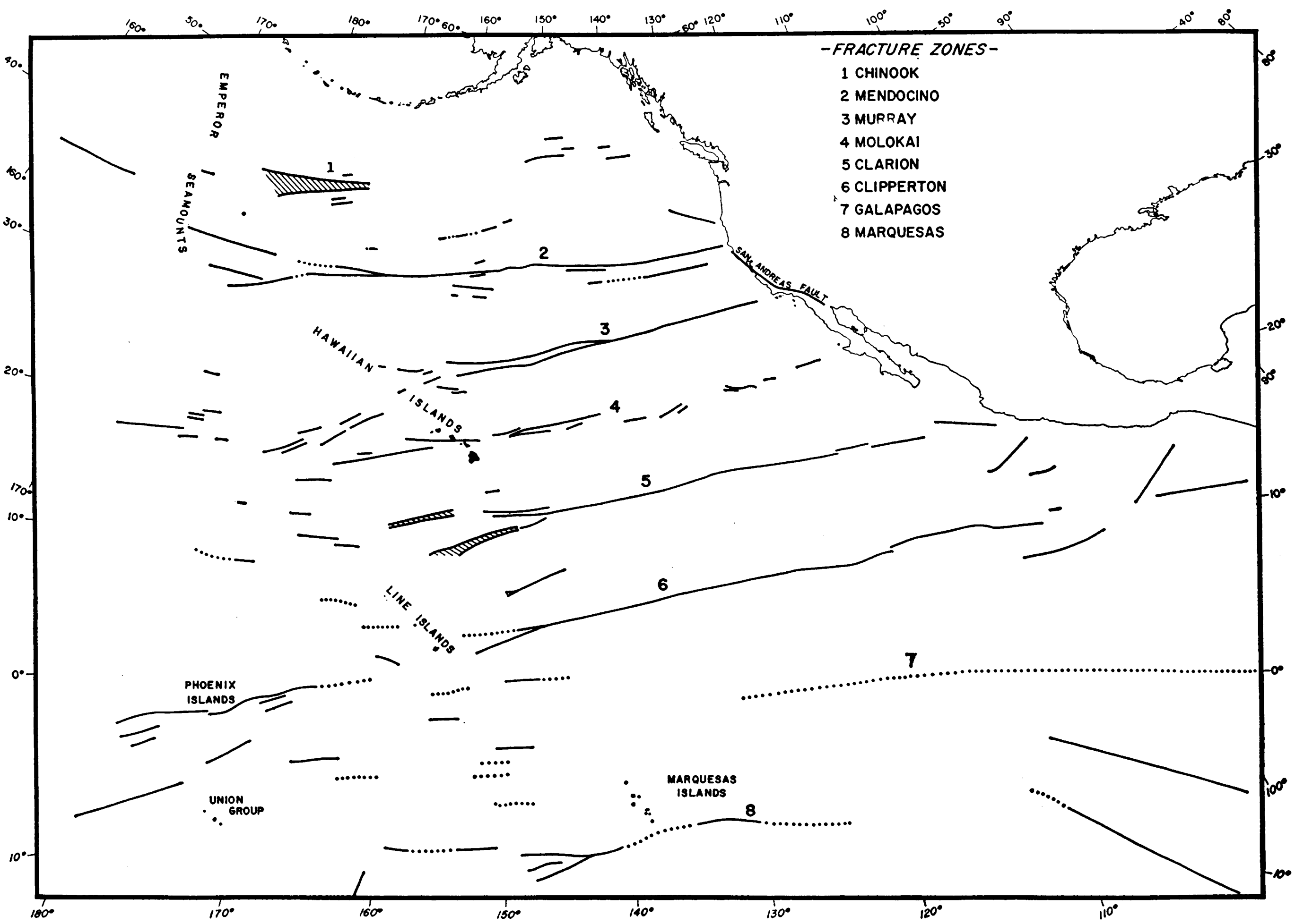

Fig. 2. Principal fracture zones of the northeastern and central Pacific; great-circle projection. A straight line on this projection is part of a true great circle.

ever, the line lies several thousand kilometers west of the edge of the visible rise as defined by bathymetry.

If one measures from the crest of the rise, the Clipperton, Clarion, and Molokai zones branch at a distance of 4600 to 4900 km. The crest is concealed under North America east of the Murray and Mendocino zones, but the position may be estimated as the center of Tertiary uplift of the western United States (*7*). Branching of these two fracture zones occurs 4500 to 4600 km west of this crest.

It may be significant that great lines of volcanoes commonly occur in the central region of branching fracture zones, where rotation of crustal blocks and tension faults would be expected. Volcanoes occur throughout the Pacific, but very large ones are mostly west of the line of branching. The southern Hawaiian Islands clearly are affected by faulting along the Molokai fracture zone because vulcanism is localized along east-west trends (*8*). A similar effect occurs on the west side of the central Hawaiian and Line islands, where narrow volcanic ridges follow fracture-zone trends. However neither the Hawaiian Island ridge nor the Molokai fracture zone is offset at their intersection (*9*). The lines of central-Pacific volcanoes apparently were superimposed on the fracture zones, which generally are buried where they intersect archipelagic aprons and volcanic ridges.

The origin and history of these great fracture zones are not becoming more obvious as additional facts accumulate. Indeed it has become necessary to distinguish them as "great" because a different system of shorter, more closely spaced, seismically active fracture zones with various trends exists in the same region along the crest of the East Pacific Rise. The probability that the great fracture zones are genetically related to the East Pacific Rise seems stronger when one considers the new evidence that branching occurs at a relatively uniform distance from the crest. However, there are at least two other possibilities: Perhaps the fracture zones of the central Pacific are a different system which intersects the northeastern-Pacific system to form what are here interpreted as branches. Perhaps the zones are part of an intermittently rejuvenated global fracture pattern of great antiquity. The extraordinary Clipperton fracture zone, which follows a great circle for a quarter of Earth's circumference, is especially extraordinary if it was produced by a nonglobal deformation.

A great fracture zone is not difficult to trace by special survey, provided a location and trend are known. Echo sounders, magnetometers, and subbottom profilers all can be used for the purpose at or near cruising speeds. Present concepts of large-scale tectonics might be more firmly based if the known fracture zones of the Pacific, Atlantic, and Indian oceans were traced to their terminations—apparently a valid purpose for the continuing Upper Mantle Project.

H. W. MENARD
Institute of Marine Resources and
Scripps Institution of Oceanography,
University of California, San Diego

References and Notes

1. H. W. Menard, *Bull. Geol. Soc. Amer.* **64**, 1149 (1955).
2. H. H. Hess, *Submarine Geology and Geophysics* (Butterworths, London, 1965), p. 322; H. W. Menard, *J. Geophys. Res.* **71**, 682 (1966); A. Malahoff, W. E. Strange, G. P. Woollard, *Science* **153**, 521 (1966).
3. By expeditions of Scripps Inst. of Oceanography.
4. Principally by U.S. Navy Oceanographic Office, Coast and Geodetic Survey, American Telephone and Telegraph Co., and Cable Wireless, Ltd.
5. H. W. Menard, *Marine Geology of the Pacific* (McGraw-Hill, New York, 1964).
6. J. T. Wilson, *Nature* **207**, 907 (1965).
7. A. J. Eardley, *Structural Geology of North America* (Harper and Row, New York, 1962).
8. A. Malahoff, W. E. Strange, G. P. Woollard, *Science* **153**, 521 (1966).
9. H. W. Menard, *J. Geophys. Res.* **71**, 682 (1966).
10. Work at sea broadly supported by ONR and NSF. Study supported by NSF contract NSF-gp-4235. I thank T. E. Chase for help in analyzing echograms. Contribution (new series) from Scripps Institution of Oceanography.

7 October 1966

Lunar Orbiter Ranging Data: Initial Results

Abstract. *Data from two Lunar Orbiter spacecraft have been used to test the significance of corrections to the lunar ephemeris. Range residuals of up to 1700 meters were reduced by an order of magnitude by application of the corrections, with most of the residuals reduced to less than 100 meters. Removal of gross errors in the ephemeris reveals residual patterns that may indicate errors in location of observing stations, as well as the expected effects of Lunar nonsphericity.*

One of the experimental missions of the Lunar Orbiter spacecraft is the providing of range data with an accuracy of 10 m, the highest accuracy yet achieved at such a great distance from Earth. These data have been used to confirm the validity of corrections now being made to the Lunar ephemeris (*1*). This confirmation consists of the order-of-magnitude reduction of the residuals (observed − computed) in range when the corrections are introduced. If the old ephemeris is used, the root mean square (r.m.s.) residual is about 800 m, with a maximum near 1700. After the corrections are applied, the r.m.s. residual is reduced to about 110 m, which is well within the uncertainties expected due to other factors. With the residuals thus reduced, the variations produced by errors due to station location and by the harmonics in the Lunar gravitational potential can be expected to exhibit a dominating influence. This, in turn, will facilitate the use of the range data for the better determination of the figure of the Moon and for the location of tracking stations.

Orbit determination of range data from Lunar Orbiter I and II gave nonrandom residuals which often far exceeded those expected from known effects. These analyses were performed with the standard Jet Propulsion Laboratory ephemeris tapes (*2*), in which the Lunar ephemeris is based on the improved Brown lunar theory [Eckert, Jones, and Clark (*3*)]. Such an ephemeris is subject to several corrections, and one of us (Mulholland) has been directing the effort to calculate and apply these corrections to the JPL ephemeris, in an effort to improve its adequacy. The simultaneous availability of the Lunar Orbiter data and the computations of the ephemeris corrections presented us with the means to test the significance of the corrections and, at the same time, to remove much of the model error for further data analysis.

Before the comparisons are examined, we will give a short explanation of how ranging data from a spacecraft in orbit around the Moon can provide an independent test of the lunar ephemeris, as well as a brief discussion of the causes from which the ephemeris corrections arise.

In the orbit determination program used for the Lunar Orbiter calculations, the selenocentric (that is, Moon-cen-